

Alma Mater Studiorum Università di Bologna
Archivio istituzionale della ricerca

Role of interface/border traps on the threshold voltage instability of SiC power transistors

This is the final peer-reviewed author's accepted manuscript (postprint) of the following publication:

Published Version:

Volosov V., Cascino S., Saggio M., Imbruglia A., Di Giovanni F., Fiegna C., et al. (2023). Role of interface/border traps on the threshold voltage instability of SiC power transistors. SOLID-STATE ELECTRONICS, 207, 1-4 [10.1016/j.sse.2023.108699].

Availability:

This version is available at: <https://hdl.handle.net/11585/954852> since: 2024-02-21

Published:

DOI: <http://doi.org/10.1016/j.sse.2023.108699>

Terms of use:

Some rights reserved. The terms and conditions for the reuse of this version of the manuscript are specified in the publishing policy. For all terms of use and more information see the publisher's website.

This item was downloaded from IRIS Università di Bologna (<https://cris.unibo.it/>).
When citing, please refer to the published version.

(Article begins on next page)

This is the post-print version of the manuscript:

Role of interface/border traps on the threshold voltage instability of SiC power transistors.

The final published version is available online at:

<https://doi.org/10.1016/j.sse.2023.108699>

© [2023]. This manuscript version is made available under the Creative Commons Attribution-NonCommercial-NoDerivs (CC BY-NC-ND) 4.0 International License (<http://creativecommons.org/licenses/by-nc-nd/4.0/>)

Role of interface/border traps on the threshold voltage instability of SiC power transistors

V. Volosov¹, S. Cascino², M. Saggio², A. Imbruglia², F. Di Giovanni², C. Fiegna¹, E. Sangiorgi¹, A.N. Tallarico¹

¹ARCES-DEI, University of Bologna, Campus of Cesena, 47521, Cesena, Italy

²STMicroelectronics, SRL, Stradale Primosole 50, 95121, Catania, Italy

Corresponding author: vladislav.volosov2@unibo.it

Abstract

In this paper the role of interface/border defects on the threshold voltage drift (ΔV_{TH}) of SiC power MOSFETs has been investigated by means of slow and fast positive bias temperature instability (PBTI), hysteresis and conductance tests. Results have shown an opposite temperature (T) dependency based on the level of the applied gate bias (V_G) and on the adopted stress technique. With $V_G > 30$ V and a slow-PBTI procedure, the creation of new oxide defects and/or the charge trapping in deep states occurs, showing a positive T-dependency. On the contrary, with a lower V_G and a fast-PBTI test, the ΔV_{TH} shows a negative T-dependency, associated to dominant role of pre-existing interface and/or border traps.

Keywords

SiC MOSFET, threshold voltage instability, hysteresis, interface/border traps, conductance, TCAD simulation.

Introduction

Silicon carbide (SiC) technology features several advantages with respect to its Silicon (Si) competitor, e.g., higher operating voltages, safer operating temperatures and higher switching frequencies. This set of features gives rise to power devices with a better trade-off between performance and robustness, ensuring their widespread application in power electronics [1].

However, from reliability stand point, it is not as stable as Si counterpart. Numerous papers have reported that SiC devices exhibit higher threshold voltage (V_{TH}) instability and faster V_{TH} recovery effects than Si-based devices [2-4], mainly ascribed to SiC/SiO₂ interface defects [5].

In [6], the ΔV_{TH} under gate bias stress has been ascribed to two separate trapping mechanisms: i) near-interface (also referred as border) oxide charge trapping due to tunneling mechanisms from SiC semiconductor [7]; ii) charge trapping in intrinsic defects at the SiO₂/SiC interface.

In [8], the adoption of slow test procedures has shown that the change in V_{TH} can be associated to capture/release of charge carriers to/from border traps, reporting, however, a significant V_{TH} recovery when a fast measurement is adopted. In addition, the V_{TH} shift decreases by increasing the temperature (T), indicating that electron emission from traps is temperature activated. Accordingly, a T-dependent

V_{TH} recovery, i.e. faster by increasing T, has been reported also in [9].

Finally, the role of the border traps on the V_{TH} instability/hysteresis has been modeled in [10] and [11] by adopting a two-stage and a four-stage non-radiative multi-phonon model, respectively.

Overall, the adoption of a proper test procedure to evaluate the V_{TH} instability and the characterization/modeling of interface/border defects is of paramount importance to fully exploit the potential of SiC-based technology.

In this work, the ΔV_{TH} induced by different PBTI test procedures (slow and fast) has been investigated, highlighting two opposite temperature dependencies. Moreover, interface defects have been characterized by means of conductance method and their effect has been modeled by TCAD simulator, qualitatively reproducing the V_{TH} hysteresis.

Results and Discussion

SiC power MOSFETs fabricated by STMicroelectronics for automotive applications [12], with a class voltage of 650 V and a typical V_{TH} of 3.2 V, have been adopted for this investigation.

First, slow PBTI tests were conducted according to JEDEC JEP184 standard [13], which consists in a measure-stress-measure technique, adopting a conditioning procedure to stabilize the V_{TH} readout, thus ensuring the same charging state of the interface traps during the characterization phases. With this approach, a full I_D - V_G measurements are carried out, hence the interface trap density (ΔD_{it}) can be calculated from subthreshold slope [14] as follows:

$$\Delta D_{it} = \frac{C_{ox}}{\ln(10) \cdot q \cdot k \cdot T} \cdot (S_i - S_0) \quad (1)$$

where C_{ox} , q , k , T and S are the gate oxide capacitance per unit of area, the elementary charge, the Boltzmann's constant, the temperature and the sub-threshold swing (1/slope), respectively.

The ΔV_{TH} at different temperatures in the case of $V_G = 20$ V and 35 V, measured by means of slow PBTI test is reported in Fig. 1. In both cases, it is mainly ascribed to charge trapping in the oxide, since, as reported in Fig. 2, the interface trap density, calculated from subthreshold slope (1), is negligible during the stress. Once excluded the role of D_{it} , the oxide trap density can be calculated as follows:

$$\Delta N_{ox} = \frac{C_{ox} \cdot \Delta V_{TH}}{q} \quad (2)$$

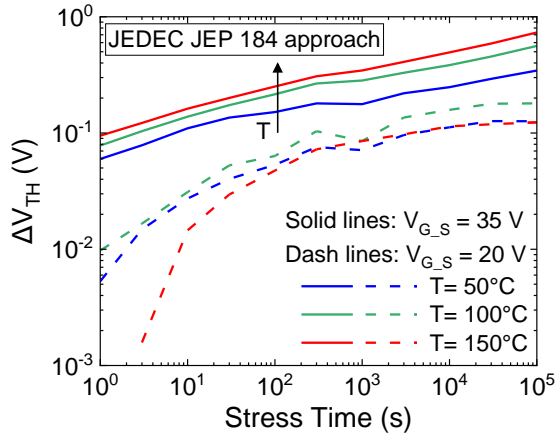


Fig. 1: ΔV_{TH} during the stress time as a function of different temperatures and $V_{G,S}$, monitored by slow-PBTI technique.

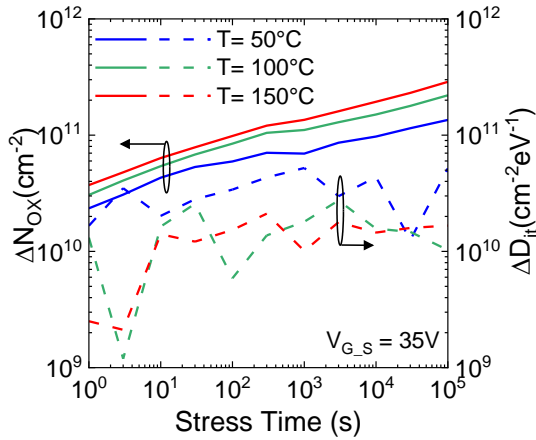


Fig. 2: ΔN_{OX} (Solid lines) and ΔD_{it} (Dash lines) calculated from ΔV_{TH} and subthreshold slope, respectively, in the case of slow-PBTI test. D_{it} refers only to slow interface states.

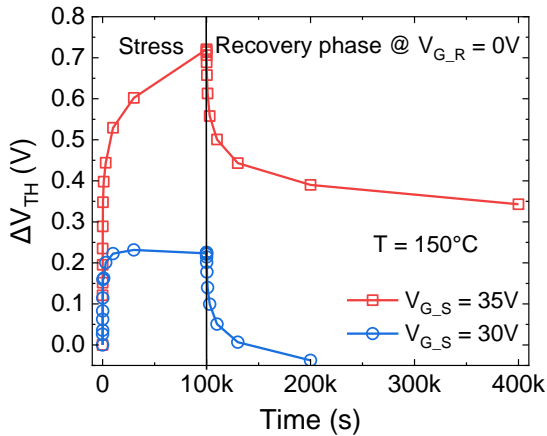


Fig. 3: ΔV_{TH} during the stress and recovery time as a function of different V_G , monitored by slow-PBTI technique. Recovery condition: $V_G = 0V$, $T = 150^\circ C$.

By observing Fig. 1, a clear and positive temperature trend is reported only in the case of $V_G = 35 V$. By applying such a high V_G , the creation of new oxide defects or the charge trapping in deep states may occur, exhibiting the usual positive

temperature dependency observed also in the case of Si-based devices. This is strengthened by Fig. 3, where a permanent or slowly recoverable ΔV_{TH} is observed after a stress at $V_G = 35 V$, despite a ~ 83 hours long recovery at $150^\circ C$. Vice versa, when a lower V_G stress is applied ($30 V$), the ΔV_{TH} is completely recovered after few hours.

In order to investigate the fast charge trapping/de-trapping mechanisms associated to interface/border defects, the fast PBTI procedure has been performed. In this case, only a portion of the I_D - V_G transfer-characteristic (from $1 V$ to $4 V$) is measured during the characterization phase and the V_{TH} readout takes just a few μs , limiting, as much as possible, fast recovery mechanisms.

Fig. 4 shows ΔV_{TH} as a function of temperature in the case of $V_G = 10 V$ and adopting the Fast PBTI test. The relatively low V_G was limited by instrument compliance (Keysight B1530A). From Fig. 4, it is possible to notice two aspects: i) although the applied V_G stress is lower than the one adopted in the case of slow PBTI (Fig. 1), the observed ΔV_{TH} is larger. The latter is completely recoverable in a few seconds as reported in Fig. 5; ii) a negative temperature dependency shows up.

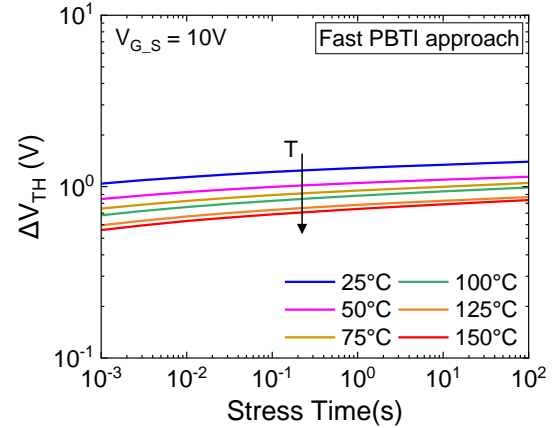


Fig. 4: ΔV_{TH} during the stress time as a function of different temperatures, monitored by fast-PBTI technique. Contribution of fast interface/border traps is included.

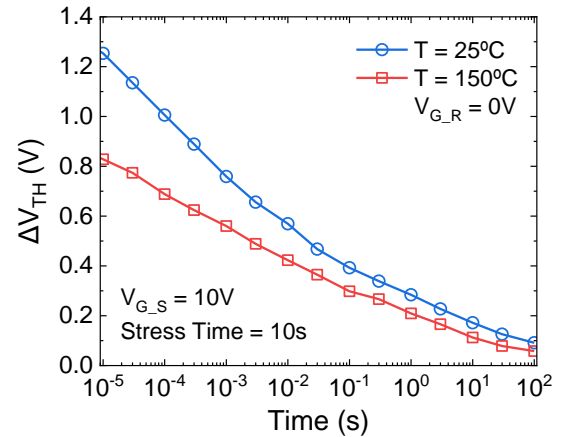


Fig. 5: ΔV_{TH} during the recovery after 10 s of stress with $V_G = 10 V$ in the case of $T = 25^\circ C$ and $T = 150^\circ C$.

By combining such aspects, a dominant role of charge trapping in pre-existing interface and/or border traps is suggested. On one hand, a faster characterization phase allows the evaluation of the ΔV_{TH} induced by (fast) defects with short capture and emission time (from μs to ms), thus obtaining a larger ΔV_{TH} . On the other hand, the higher temperature induces a faster recovery mechanism, showing up a negative temperature dependency. A similar T-dependency has been reported in [9] and [10] for interface and border traps, respectively.

To confirm the presence of fast interface/border traps, hysteresis measurements have been carried out

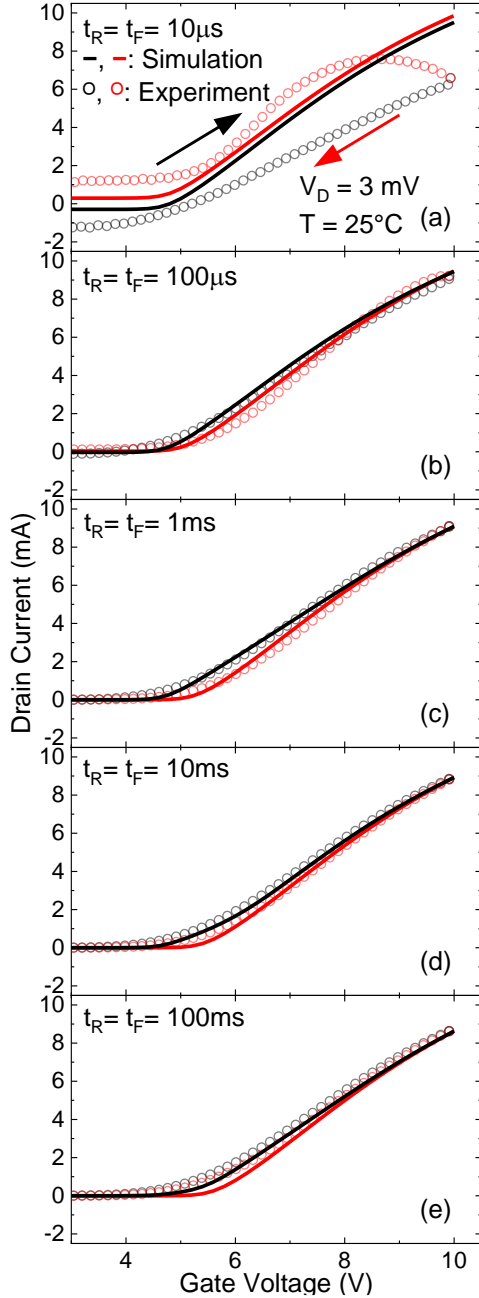


Fig. 6: Measured (symbols) and simulated (lines) $I_D V_G$ characteristics with related V_{TH} hysteresis under different sweeping rates. From 0 V to 10 V in (a) 10 μs , (b) 100 μs , (c) 1 ms, (d) 10 ms, and (e) 100 ms.

at 25°C by adopting different sweeping rates. In particular, V_G was swept from 0 V to 10 V and back to 0 V with sweeping times ranging from 10 μs to 100 ms, while V_D was kept constant.

The experimental $I_D V_G$ and related hysteresis are reported in Fig. 6 (symbols). The V_{TH} hysteresis, although quite limited, confirms the presence of fast interface defects. It is worth noting that the negative V_{TH} hysteresis observed in the case of 10 μs sweep time is an artifact of the measurement. In particular, since the drain voltage (V_D) was limited due to current compliance of the instrument, the related current was affected by the displacement gate current of the large-area device.

The conductance method has been adopted to measure the interface trap density (D_{it}). It is based on measuring the equivalent parallel conductance (G_P) of a MOS structure, representing the loss mechanism due to interface trap capture and emission of carriers [14]. In particular, by considering traps with energy continuously distributed throughout the SiC bandgap, D_{it} can be calculated as follows:

$$D_{it} \approx \frac{2.5}{q} \left(\frac{G_P}{\omega} \right)_{\max} \quad (3)$$

The conductance (G_P/ω) measured as a function of frequency ($\omega = 2\pi f$) is shown in Fig. 7 for different temperatures. The show up of two peaks (A and B) suggests the presence of defects with different features, including emission/capture times, activation energy (E_A) and concentration. By performing conductance measurements with different V_G and T , the interface trap density D_{it} as a function of E_A ($E_T - E_C$) has been calculated for the two defects and reported in Fig. 8 (symbols).

The relatively limited energy range of D_{it} may be ascribed to conductance method, since it yield D_{it} only in the portion of the bandgap scanned by the Fermi level in depletion and weak inversion conditions.

TCAD simulator [15] has been adopted to verify the electrostatic effect of such traps on the $I_D V_G$ characteristics of the SiC power MOSFET.

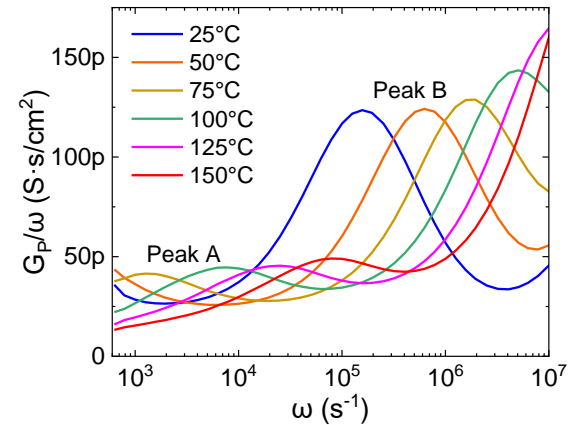


Fig. 7: G_P/ω versus ω as a function of different temperatures, measured using Conductance method.

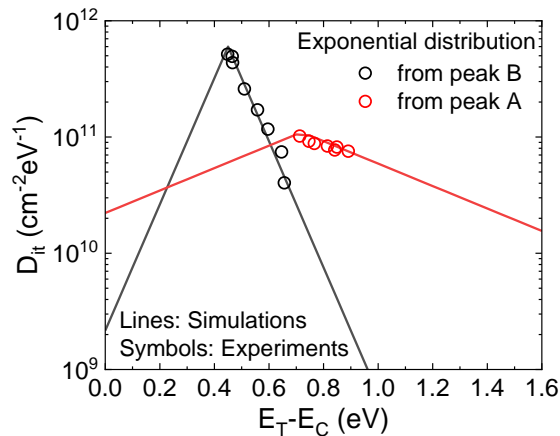


Fig. 8: Interface trap density as a function of energy position, calculated from conductance experiments (symbols) and adopted for in the simulations (lines).

Based on the experiments, two exponential trap distributions have been added at the SiC/SiO₂ interface as reported by lines in Fig. 8. Their adoption allows us to qualitatively reproduce the V_{TH} hysteresis observed during tests with different V_G sweep rates (lines, Fig. 6), confirming the important role of interface defects on the V_{TH} instability. However, it is worth noting that such distributions are not sufficient to reproduce the ΔV_{TH} reported in Fig. 4, as it is the result of interface, border and oxide traps. The last two are difficult, if not impossible, to characterize with conductance measurements.

Conclusion

The role of interface/border defects on the V_{TH} instability has been investigated by means of slow-, fast-PBTI and hysteresis tests. Adopting the proper test procedure is of paramount importance, since the results can be completely different. A slow-PBTI procedure allows to mainly evaluate the effect of oxide charge trapping on the ΔV_{TH} , which has a positive T-dependency. Vice versa, a negative T-dependency is observed when a fast-PBTI test is adopted, since the role of D_{it} and border traps becomes dominant. Finally, D_{it} has been characterized and their effect on the V_{TH} hysteresis has been qualitatively reproduced by means of TCAD simulator.

Acknowledgment

This work is partly funded by TRANSFORM, a European co-funded innovation project granted by the ECSEL Joint Undertaking (JU) under grant agreement No. 101007237.

References

[1] J. Biela et al., "SiC versus Si—Evaluation of Potentials for Performance Improvement of Inverter and DC–DC Converter Systems by SiC Power Semiconductors", *IEEE Trans. Ind. Electron.*, vol. 58, no. 7, pp. 2872–2882, July 2011, doi: 10.1109/TIE.2010.2072896.

[2] K. Puschkarsky et al., "Review on SiC MOSFETs High-Voltage Device Reliability Focusing on Threshold Voltage Instability", *IEEE Trans. Electron Devices*, vol. 66, no. 11, pp. 4604–4616, Nov. 2019, doi: 10.1109/TED.2019.2938262.

[3] A.K. Ghosh et al., "Threshold-voltage bias-instability in SiC MOSFETs: effects of stress temperature and level on oxide charge buildup and recovery", *Semicond. Sci. Technol.*, vol. 37, no. 7, 2022, doi: 10.1088/1361-6641/ac606c.

[4] T. Aichinger et al., "Threshold voltage peculiarities and bias temperature instabilities of SiC MOSFETs", *Microelectron. Reliab.*, 80, pp. 68–78, 2018, doi: 10.1016/j.microrel.2017.11.020.

[5] D. Cornigli et al., "Characterization and Modeling of BTI in SiC MOSFETs", *IEEE 49th European Solid-State Device Research Conference (ESSDERC)*, pp. 82–85, Cracow, Poland, 2019, doi: 10.1109/ESSDERC.2019.8901761.

[6] P. Fiorenza et al., "Identification of two trapping mechanisms responsible of the threshold voltage variation in SiO₂/4H-SiC MOSFETs", *Appl. Phys. Lett.*, 117, 103502 (2020); <https://doi.org/10.1063/5.0012399>.

[7] A. J. Lelis et al., "SiC MOSFET threshold-stability issues", *Materials Science in Semiconductor Processing*, vol. 78, pp. 32–37, May 2018, doi: 10.1016/j.mssp.2017.11.028.

[8] A. Ghosh et al., "Studies of Bias Temperature Instabilities in 4H-SiC DMOSFETs", *IEEE International Reliability Physics Symposium (IRPS)*, Dallas, TX, USA, 2020, pp. 1–4, doi: 10.1109/IRPS45951.2020.9128318.

[9] M. Cioni et al., "Identification of Interface States responsible for V_{TH} Hysteresis in packaged SiC MOSFETs", *IEEE International Reliability Physics Symposium (IRPS)*, Dallas, TX, USA, 2022, pp. 5B.3.1–5B.3.6, doi: 10.1109/IRPS48227.2022.9764543.

[10] A. Vasilev et al., "TCAD Modeling of Temperature Activation of the Hysteresis Characteristics of Lateral 4H-SiC MOSFETs", *IEEE Trans. Electron Devices*, vol. 69, no. 6, pp. 3290–3295, June 2022, doi: 10.1109/TED.2022.3166123.

[11] G. Carangelo et al., "TCAD modeling of bias temperature instabilities in SiC MOSFETs", *Solid-State Electronics*, Vol. 185, 2021, 108067, doi: 10.1016/j.sse.2021.108067.

[12] www.st.com/en/power-transistors/sctwa35n65g2v4ag.html

[13] JEDEC JEP 184, Guideline for evaluating Bias Temperature Instability of Silicon Carbide Metal-Oxide-Semiconductor Devices for Power Electronic Conversion, Mar. 2021.

[14] D. K. Schroder, "Semiconductor Material and Device Characterization", Third edition, John Wiley & Sons, 2006, ISBN No. 13:978-0-471-73906-7.

[15] Sentaurus-Device User Guide, v.U-2022.12, Synopsys Inc., 2022.